



Improved cell activity on biodegradable photopolymer scaffolds using titanate nanotube coatings



S. Beke^{a,*}, R. Barenghi^b, B. Farkas^a, I. Romano^a, L. Kőrösi^c, S. Scaglione^b, F. Brandi^{a,d}

^a Nanophysics, Istituto Italiano di Tecnologia, Via Morego 30, 16163 Genova, Italy

^b IELIT, National Research Council (CNR), Via De Marini 6, 16149 Genova, Italy

^c Department of Biotechnology, Nanophage Therapy Center, Enviroinvest Corporation, Kertváros u. 2, H-7632 Pécs, Hungary

^d Istituto Nazionale di Ottica, CNR, Via G. Moruzzi 1, 56124-Pisa, Italy

ARTICLE INFO

Article history:

Received 10 March 2014

Received in revised form 30 March 2014

Accepted 1 July 2014

Available online 9 July 2014

Keywords:

Laser photocuring

Scaffolds

Titanate nanotubes

Tissue engineering

Cell culturing

Excimer laser

ABSTRACT

The development of bioactive materials is in the premise of tissue engineering. For several years, surface functionalization of scaffolds has been one of the most promising approaches to stimulate cellular activity and finally improve implant success. Herein, we describe the development of a bioactive composite scaffold composed of a biodegradable photopolymer scaffold and titanate nanotubes (TNTs). The biodegradable photopolymer scaffolds were fabricated by applying mask-projection excimer laser photocuring at 308 nm. TNTs were synthesized and then spin-coated on the porous scaffolds. Upon culturing fibroblast cells on scaffolds, we found that nanotubes coating affects cell viability and proliferation demonstrating that TNT coatings enhance cell growth on the scaffolds by further improving their surface topography.

© 2014 Elsevier B.V. All rights reserved.

1. Introduction

Tissue engineering aims to repair and replace lost or damaged tissues by inducing a specific cellular response according to the chemical–physical cues provided by the implanted materials [1]. Ideally, the scaffold design is aimed at reproducing all required signals at macro-, micro- and nanoscales to foster and direct cellular attachment, proliferation, and desired differentiation towards specific cell phenotypes. In this respect, nanoscale surface properties are fundamental to enhance cell–substrate interaction [2,3], and nanostructures offer the possibility to further functionalize the substrates through a biomimetic approach [4–9].

Nanostructures, e.g. nanoparticles and nanotubes, can also be applied as drug delivery systems and thereby be a potential matrix for various therapeutic inductions. Their volume can be filled with chemicals, drugs, and biomolecules [10]. Surface nanostructures can also be used for more efficient and precise nano-sized delivery compared to conventional approaches [11–15].

Nanotubular titania (TiO₂) surfaces have been recently proposed as alternative architectures to enhance the interaction between the implant and living matter or biological species. In particular, it was demonstrated that titanium oxide nanotubes enhance growth rates and

bone forming ability as well as accelerate osteogenic differentiation of mesenchymal stem cells [11,15]. Moreover, it was shown that titanium oxide-based materials adopted as bone implants might affect in vivo cell adhesion, osteointegration, and finally, bone regeneration [11,16]. For these reasons, they have been widely investigated as bioactive substrates to improve the osteoconductivity of orthopedic implants, finally enhancing the apposition of bone from existing bone surfaces and stimulate new bone formation [17,18].

Besides their chemical composition, high attention has been paid to the nanotubes' diameters which may influence the functionality and the activity of osteoblasts [11,19,20]. In particular, as the nanotube diameter increases, the osteogenic biochemical activity also increases, reaching the best values on 100 nm-diameter nanotubes [11,19,20]. By varying the diameter sizes, the location and spacing of transmembrane integrins change, thus cytoskeletal tensions in the actin filaments and in the adhering cells are affected differently.

Although both the nature of cell adhesion and the degree of cytoskeletal tension affect the cell response, the precise role of nanotopography on the adhesion, morphology, and differentiation of cells has not been established yet [11].

TiO₂ nanotubes have the capability to change the adsorption of extracellular matrix (ECM) proteins, such as fibronectin, laminin, and bovine serum albumin and mesenchymal stem cell (MSC) attachment if subjected to a change in their wetting behavior [19]. In particular, nanotubes turn from super-hydrophilic (as prepared) to super-hydrophobic after the addition of a self-assembled

* Corresponding author.

E-mail address: szabolcs.beke@iit.it (S. Beke).

monolayer (octadecylphosphonic acid) [11]. Differences in hydrophobicity were found to be diameter dependent, too. It is important to note that in the super-hydrophobic case the adhesion is diameter-independent, while in the case of super-hydrophilic surface the adhesion is diameter-dependent [11,16].

In this article, we report on cell culture experiments using fibroblast cells on bioactive composite scaffolds. The scaffolds are biodegradable photopolymer scaffolds functionalized with titanate nanotubes (TNTs). In a previous paper [21], we reported on the development of a rapid process to produce rigid biodegradable photopolymer scaffolds using excimer laser photocuring of a synthetic biopolymer: poly(propylene fumarate)/diethyl fumarate blend (PPF:DEF, 7:3 w/w). We also investigated high-resolution photocuring of PPF:DEF using a laser wavelength of 248 nm [22], and performed a comparative study between the two laser wavelengths at 248 nm and 308 nm [23]. We recently introduced our novel method, called mask projection excimer laser stereolithography [24], being a versatile and accurate technique to fabricate 3D scaffolds with controlled architecture. Its capability is showcased in that paper by a variety of mm-sized biodegradable scaffolds with a high spatial resolution well-suited for tissue engineering applications.

Among polymeric materials, PPF-based scaffolds display satisfactory properties in terms of biocompatibility, mechanical properties, sterilizability [25], and handling characteristics making them a promising alternative to traditional substitutes for autologous or allograft bones [26]. In [25] we presented the biodegradability of the material used for this study.

The combination of laser-produced PPF-based scaffolds and spin-coated TNT films was presented in a previous study [27] being a facile production of a novel material made of a PPF:DEF scaffold coated with additive-free TNTs. The structure and the morphological properties of the resulting hybrid scaffolds were discussed. Here we investigate the role of TNT functionalization on cellular activity at early period of cell culture *in vitro*.

2. Experimental

2.1. Synthesis of TNTs and polymer

The synthesis of TNTs was similar as described in [28]. 0.5 g of Degussa P25 TiO₂ was dispersed in 15 mL of 10 M aqueous NaOH solution and the resulting dispersion was transferred to a Teflon-lined autoclave. The autoclave was heated at 150 °C for 12 h (*p* ~ 4.7 bar) without stirring. After the hydrothermal reaction, the alkaline dispersion was washed with water until the pH decreased to ~ 11, and then 0.1 M aqueous H₃PO₄ solution was added to decrease the pH further to 6. The acid treatment was carried out for 12 h at room temperature and then the system was centrifuged. The obtained sediment was washed with water and then ethanol. The washing procedure with ethanol was continued via centrifugation at 12,000 rpm. The resulting supernatant (the stable TNT sol) was collected.

PPF was synthesized as reported in [29]. Briefly, a condensation reaction was conducted between fumaric acid and propylene glycol, with a molar ratio of 0.8. In a triple-neck flask with an overhead mechanical stirrer, a thermometer and a Barrette trap connected beneath the condenser, the reaction was conducted in 140 °C for 16–17 h and then in 180–190 °C for 4–5 h. During the first period of the reaction, water was collected as byproduct, then with an increasing temperature the unreacted propylene glycol and low molecular weight impurities were removed. After keeping the product at room temperature overnight, it was possible to purify it by rotary evaporation in CH₂Cl₂. Finally, PPF was blended with DEF in ratio 7:3 and 1% photoinitiator (Bapo) was added to the polymer resin.

The schematic of the experimental apparatus used for high-resolution photocuring experiments is shown in [21]. The light source is a XeCl excimer laser at 308 nm with laser pulse duration of 20 ns

and repetition rate of 1–100 Hz (CompexPro 110). The mask image is projected on the target using a demagnification of 4.

2.2. TNT coatings on the scaffolds

TNT-coated scaffolds were prepared by a spin-coating method. 50 µL of 1% TNT ethanolic sol was dropped onto the scaffolds immobilized on a 1 cm-diameter quartz substrate rotated at 3000 rpm. The as-prepared layer was subsequently dried for 30 s in the spin-coater. In order to prepare multilayer films, the above deposition step was repeated five times.

2.3. Cell seeding and culture

Samples used for the preliminary cell studies were divided in two groups: polypropylene fumarate (PPF) scaffolds either coated or not coated with TNT. Glass slides, either coated or uncoated, were used as control. All scaffolds were irradiated overnight with a UV lamp to obtain high sterility before culturing.

Mouse fibroblast cell line (3T3) was expanded in a DMEM expansion medium supplemented with 10% fetal calf serum (FCS). The culture media was changed twice a week. When the cells became confluent and reached the required number, 3T3s were enzymatically detached with 0.05% trypsin and counted. Samples were sterilized under UV lamp for 90 min and placed in a 24-well plate for cell culture. Cells were then seeded onto the surface of samples, at a density of 5×10^4 cells/cm² and a concentration of 0.5 million/mL. Samples were cultured up to one week in the incubator in an atmosphere of 5% CO₂ allowing gas exchange in the reservoir at 37 °C. After 1 and 7 days of culture, samples were washed in buffer saline solution, and the cellular adhesion/orientation and proliferation, respectively, were investigated. All experiments were performed in duplicates.

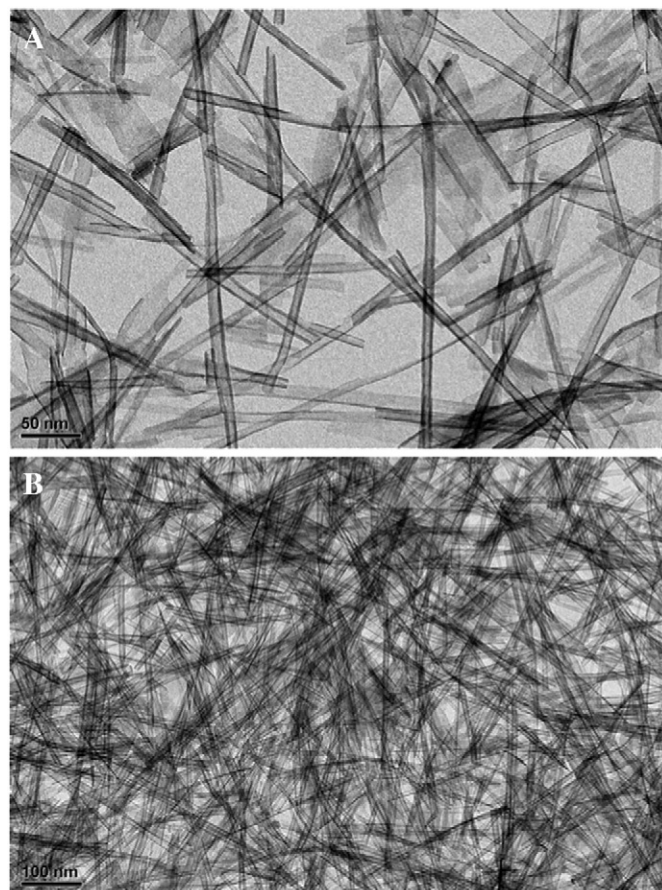


Fig. 1. TEM images of TNTs at two different magnifications.

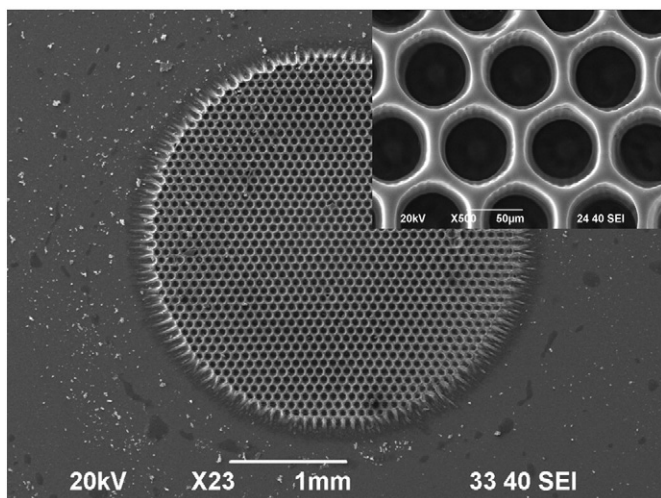


Fig. 2. SEM image of a PPF:DEF scaffold with a highlight on the porosity in the inset.

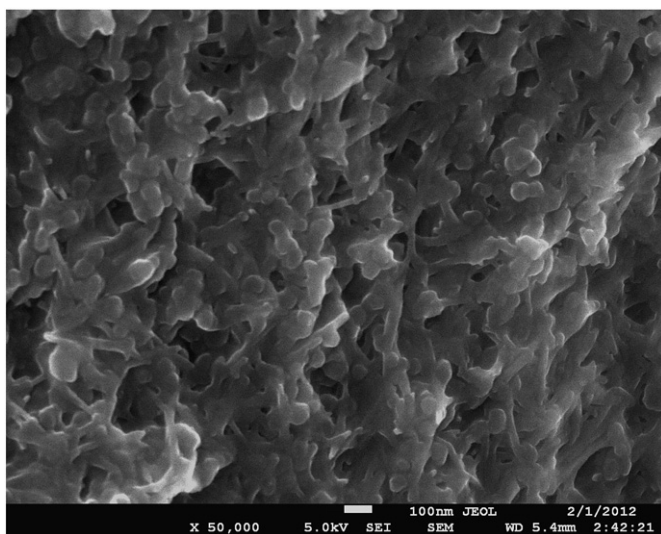


Fig. 3. SEM image of the TNT-coating on scaffold substrate showing the homogenous nanotube distribution.

2.4. Cell viability

To determine cell viability within the scaffolds, samples were stained using the Live/Dead Cell Double Staining Kit (Sigma-Aldrich) according to the manufacturer's instructions. Briefly, the samples were

incubated with the Live/Dead reagents (calcein AM for living cells and propidium iodide for dead cells) for 15 min at 37 °C, and then observed under fluorescence optical microscope. For each sample, six acquired images were processed in duplicates for each time point. An open source image analysis software (ImageJ) was used to count the number of cells, both dead and alive, by analyzing the red and green channels, respectively. Statistical evaluation was performed using non-parametric Mann–Whitney test to determine significant differences between groups. The significance level was set at $p < 0.05$. All results were presented as mean \pm standard deviation.

2.5. SEM and TEM observation

Samples were washed with phosphate-buffered saline (PBS), fixed with 4% paraformaldehyde for 1 h and washed again with PBS. Scaffolds were then dehydrated using ethanol solutions scale (70%–100%) for 5 min each and dried in air. Finally they were fixed on aluminum stubs and sputter-coated with gold. SEM images were acquired using JEOL JSM-6490 electron microscope. To analyze cell–substrate interaction, SEM analysis was carried out using a JEOL JSM 6490LV (Jeol, Tokyo, Japan) operating at 15 kV. Samples were previously sputter coated with a 10 nm thick gold film using a Cressington 208HR coating system (Cressington Scientific Instruments Inc., Watford, UK).

Transmission electron microscopy (TEM) images of the TNT were obtained with a JEOL JEM-1011 electron microscope at an accelerating voltage of 100 kV. A small amount of sol of TNT was dropped on a grid. Cellular adhesion onto TNT-coated substrate has been evaluated with high resolution imaging using a JEOL JSM 7500FA (JEOL, Tokyo, Japan) equipped with a cold FEG, operating at 5 kV acceleration voltage. Samples have been carbon coated with a 10-nm thick film using an Emitech K950X high vacuum turbo system (Quorum Technologies Ltd., East Sussex, UK).

3. Results and discussions

3.1. Structure and morphology of TNTs

TNTs were prepared by a hydrothermal method in alkaline medium at 150 °C and 4.7 bar ambient pressure [27]. The XRD pattern of TNT dried at 50 °C was presented therein [27].

In our previous study the elemental composition of TNTs was investigated by energy-dispersive X-ray spectroscopy (EDS) and beside Ti and O, Na and P elements were also detected. The atomic ratio Na:Ti was found to be 0.04, therefore the formula of TNT can be written as follows: $H_2 - xNa_xTi_2O_5 \times H_2O$ (where $x = 0.08$). The P was present in trace quantity; the atomic ratio P:Ti was as low as 0.044. Data are presented in [27].

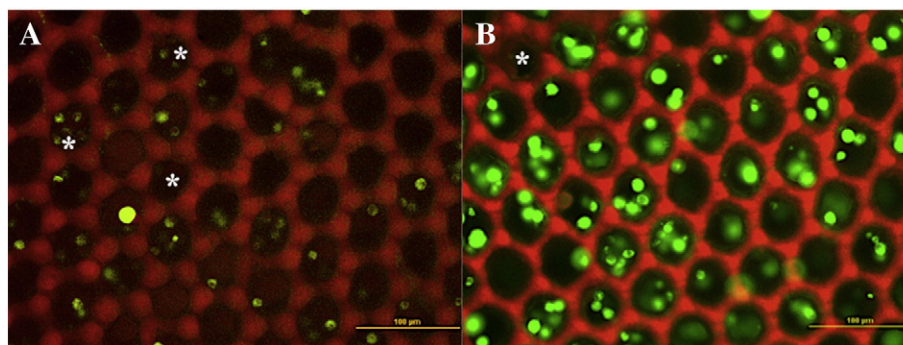


Fig. 4. Fluorescence optical microscopy images of PPF:DEF scaffolds alone (A), and on TNT-coated scaffolds (B) after 24 h of culture. The green fluorescence corresponds to live cells, and the red staining is associated with dead cells (d). The bars are 100 μ m. Stars indicate dead cells.

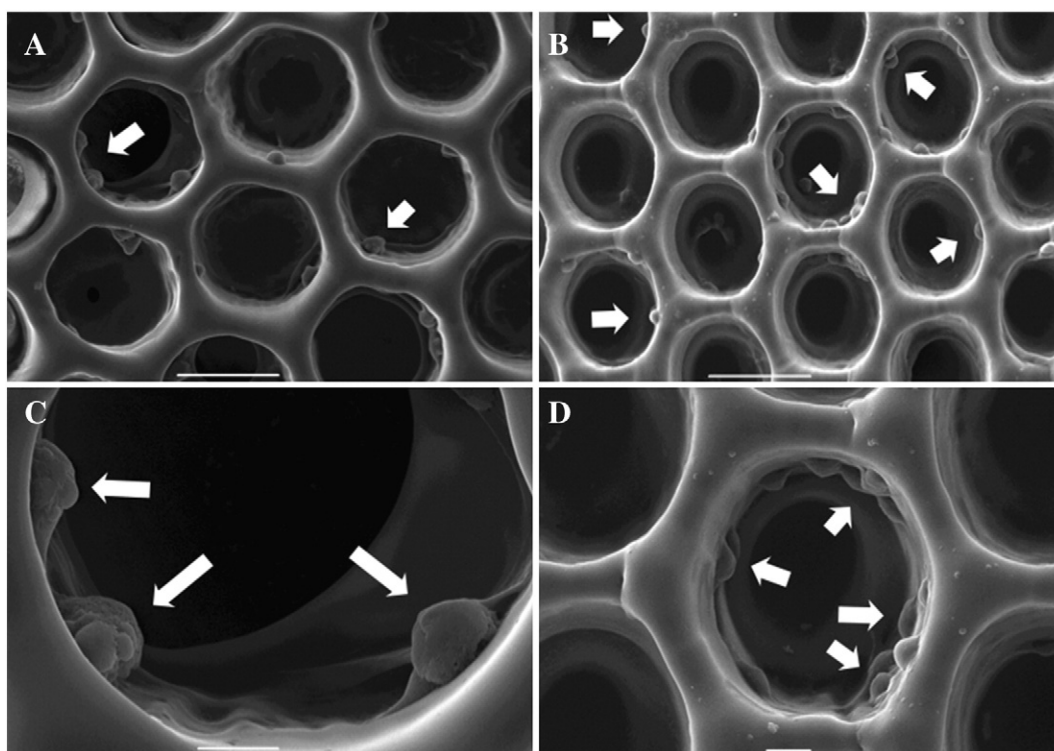


Fig. 5. Scanning electron microscopy images of cells on a scaffold alone (A, C), TNT-coated scaffold (B, D) after 24 h of culture. Arrows show cells adhering to the scaffold. The bars are 50 μm in panels A and B, and 10 μm in panels C and D.

TEM images (Fig. 1A, B) show nanotubes of about 6 nm in diameter and several hundreds of nanometers in length.

3.2. Scaffold production with TNT coating

Scaffolds with the same size (3 mm in diameter), pore dimensions (55 μm with 10 μm spacing) and porosities were employed for cell culturing as reported in our previous study [27], i.e., PPF:DEF scaffolds with round-shaped channels/pores obtained by applying 264 pulses and a laser pulse fluence of 20 mJ/cm^2 at a repetition rate of 20 Hz. A scaffold image is presented in Fig. 2 with an inset highlighting the porosity. The estimated height is about 80 μm . The laser-fabricated scaffolds were coated by TNT sols using a spin-coating method and became

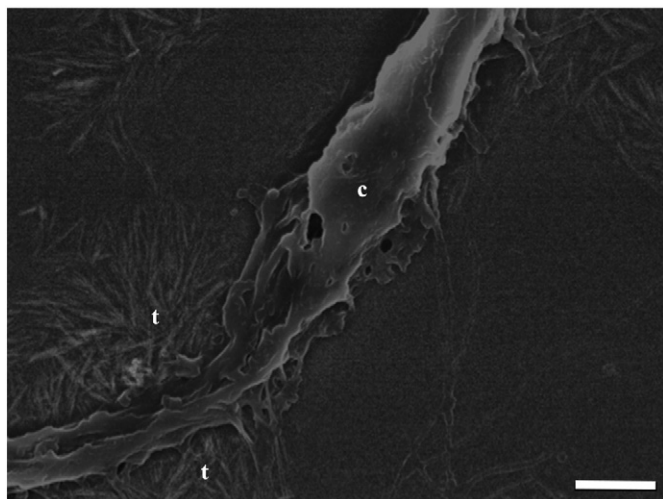


Fig. 6. SEM image of a fibroblast cell (C) on TNT-coated substrate (T) after 24 h of culture. The bar is 1 μm .

homogeneously coated with TNT (Fig. 3). The TNT morphology can be seen in Fig. 3, however, due to the necessary carbon coating used for SEM observations the tubes are covered with carbon (~ 10 nm) thus they look thicker in Fig. 3 compared to Fig. 1.

We performed elemental analysis of the TNT-coated scaffolds and proved that the TNT coatings remained stable after soaking them in 37 $^{\circ}\text{C}$ of PBS. Prior and after the soaking test, the elemental percentage of Ti was the same showing the undetached TNT layer on the scaffolds. Detailed description of this investigation can be found in [27].

3.3. Cell culturing experiments

By loading an equal number of 3T3 on all samples and 24 h of seeding, we observed a higher cell density on the TNT-coated scaffolds (Fig. 4B) compared to the control, i.e. on the scaffolds without TNT coatings (Fig. 4A).

Cell viability was investigated by double staining with both calcein-AM and propidium iodide (Fig. 4). After being double-stained, living cells emitted strong green calcein fluorescence because of esterase activity; in contrast, dead cells generated a bright red fluorescence when propidium iodide entered cells with damaged membranes.

Although the interaction between TNT and cells needs more exploration, this result highlights the role of the higher surface roughness by the TNT-functionalization, which enhances the cell-substrate interaction and cellular adhesion. Moreover, this data is in agreement with previous studies, indicating that mesenchymal stem cells cultured on TiO_2 nanotube array surface have shown more active proliferation when the nanotube diameter is below 30 nm [30,31]. However, besides the topological structure, also chemical cues provided by TNT-coated scaffolds might influence the cellular activity, offering a more biocompatible and bioactive surface for cells [32].

Interestingly, very few cells (indicated with stars) died after cell adhesion on the PPF-based scaffolds, demonstrating that neither the scaffold itself, nor the TNT is cytotoxic.

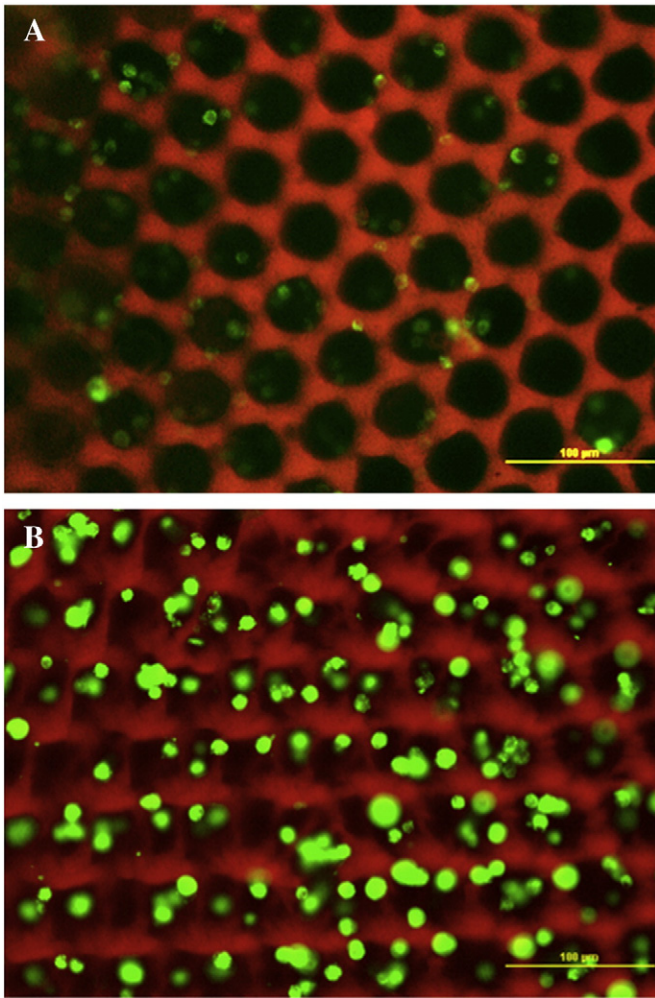


Fig. 7. Fluorescence microscopy images of scaffold alone (A) and TNT-coated scaffold (B) after 7 days of culture. The green fluorescence corresponds to live cells, and red staining corresponds to dead cells. The bar is 100 µm.

These results were also confirmed by SEM analysis (Fig. 5), where we observed that on the PPF:DEF and TNT-coated PPF:DEF scaffolds cells displayed a good interaction with the surface. As a control, cells were seeded on both TNT-coated and uncoated glass substrates, showing a good adhesion on both surfaces after 24 h.

The adhesion and spreading of cells on the material were revealed by a direct interaction between cells and TNT functionalized substrate; in particular, we observed a cytoskeleton elongation adhering to several TNT nanotubes. Fig. 6 shows a high resolution SEM image of a fibroblast cell (C) on TNT-coated substrate (T) after 24 h of culture. Scaffold properties play a pivotal role in controlling the cell growth and impose a direct influence on cell fate [33]. Cell adhesion, spreading, and proliferation represent the initial phase of cell–scaffold communication, which subsequently may affect the differentiation and mineralization. In this study, a nanostructured bioactive coating was developed to mimic the extracellular matrix, thus acting as a physical substrate for cell attachment and as a microenvironment to provide signals for cellular maturation.

Besides cell adhesion, the cell proliferation was evaluated on the samples. Fig. 7 shows cells colonizing the PPF:DEF scaffolds, coated and non-coated with TNT after 7 days of culture. Cells grow, proliferate, and form interconnections. On the TNT-coated PPF:DEF scaffolds a higher number of cells were observed in the fluorescence microscopy images compared to the uncoated substrate and a lower number of dead cells were detected.

The quantitative *in vitro* growth of cells, evaluated by dead–alive cell assay, was carried out by comparing the amount of cells measured on all scaffolds after day 1 and day 7 (Fig. 8). In particular, both coated and uncoated scaffolds displayed a statistically higher number of cells after day 7 compared to that measured on day 1 after cell seeding.

Moreover, both after day 1 and 7, there were more cells colonizing the coated scaffolds than the uncoated ones (statistically significant difference, Mann–Whitney test).

Only a few cells were found dead on the uncoated scaffolds after 7 days, while on the TNT-coated scaffolds a higher number of dead cells were measured after 7 days. That is, probably the massive presence of cells restricted the available surface for proliferation. These results confirm that functionalizing the polymeric surfaces with TNTs may positively affect cell adhesion and proliferation over time compared to the uncoated control surface.

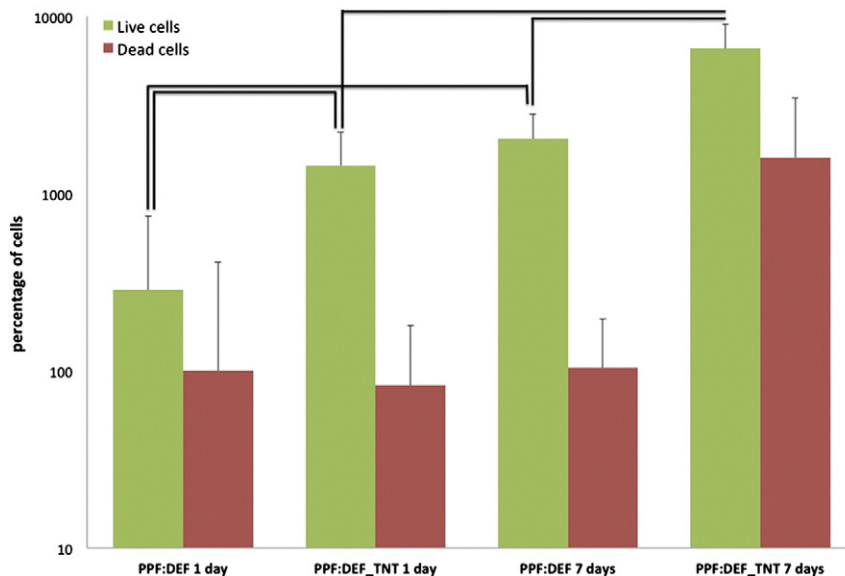


Fig. 8. Cells percentage per sample normalized to dead cells in PPF:DEF scaffolds after one day of culture. Mean and standard deviation are shown for both samples after 1 and 7 days of culture.

SEM analysis performed on all scaffolds after one week of cell culture confirmed these results (data not shown).

4. Conclusions

Biodegradable PPF:DEF scaffolds have been fabricated by excimer laser photocuring and coated with TNTs. The scaffolds with titanate coatings showed an enhanced cell growth and proliferation compared to the uncoated ones. TNT coatings are promising candidates to be utilized as biological implant coatings for tissue engineering and regenerative medicine. These reproducible platforms will be of high benefit for clinical and research applications.

Acknowledgment

The authors are thankful for Alice Scarpellini and Paola Gavazzo for assisting in SEM imaging and cell culture experiments, respectively. This work has been supported in part by the European Community (FP7-NMP-2013-EU-China) grant agreement no. 604263 (NEUROSCAFFOLDS).

Appendix A. Supplementary data

Supplementary data to this article can be found online at <http://dx.doi.org/10.1016/j.msec.2014.07.008>.

References

- [1] G. Pennesi, S. Scaglione, P. Giannoni, R. Quarto, Regulatory influence of scaffolds on cell behavior: how cells decode biomaterials, *Curr. Pharm. Biotechnol.* 12 (2011) 151–159.
- [2] M. El Fray, A.R. Boccaccini, Novel hybrid PET/DFA-TiO₂ nanocomposites by in situ polycondensation, *Mater. Lett.* 59 (2005) 2300–2304.
- [3] N. Sachot, O. Castano, M.A. Mateos-Timoneda, E. Engel, J.A. Planell, Hierarchically engineered fibrous scaffolds for bone regeneration, *J. R. Soc. Interface* 10 (2013) 20130684.
- [4] R. Gonzalez-McQuire, J.Y. Chane-Ching, E. Vignaud, A. Lebugle, S. Mann, Synthesis and characterization of amino acid-functionalized hydroxyapatite nanorods, *J. Mater. Chem.* 14 (2004) 2277–2281.
- [5] R. Intartaglia, A. Barchanski, K. Bagga, A. Genovese, G. Das, P. Wagener, et al., Bioconjugated silicon quantum dots from one-step green synthesis, *Nanoscale* 4 (2012) 1271–1274.
- [6] K. Bagga, A. Barchanski, R. Intartaglia, S. Dante, R. Marotta, A. Diaspro, et al., Laser-assisted synthesis of *Staphylococcus aureus* protein-capped silicon quantum dots as bio-functional nanoprobe, *Laser Phys. Lett.* 10 (2013).
- [7] L. Afferrante, G. Carbone, Biomimetic surfaces with controlled direction-dependent adhesion, *J. R. Soc. Interface* 9 (2012) 3359–3365.
- [8] Y. Liu, G. Wu, K. de Groot, Biomimetic coatings for bone tissue engineering of critical-sized defects, *J. R. Soc. Interface* 7 (Suppl. 5) (2010) S631–S647.
- [9] A.M. Ballo, W. Xia, A. Palmquist, C. Lindahl, L. Emanuelsson, J. Lausmaa, et al., Bone tissue reactions to biomimetic ion-substituted apatite surfaces on titanium implants, *J. R. Soc. Interface* 9 (2012) 1615–1624.
- [10] C. Von Wilmsky, S. Bauer, R. Lutz, M. Meisel, F.W. Neukam, T. Toyoshima, et al., In vivo evaluation of anodic TiO₂ nanotubes: an experimental study in the pig, *J. Biomed. Mater. Res. B Appl. Biomater.* 89B (2009) 165–171.
- [11] K.S. Brammer, C.J. Frandsen, S. Jin, TiO₂ nanotubes for bone regeneration, *Trends Biotechnol.* 30 (2012) 315–322.
- [12] E. Hirata, T. Akasaka, M. Uo, H. Takita, F. Watari, A. Yokoyama, Carbon nanotube-coating accelerated cell adhesion and proliferation on poly (L-lactide), *Appl. Surf. Sci.* 262 (2012) 24–27.
- [13] K. Gulati, S. Ramakrishnan, M.S. Aw, G.J. Atkins, D.M. Findlay, D. Losic, Biocompatible polymer coating of titania nanotube arrays for improved drug elution and osteoblast adhesion, *Acta Biomater.* 8 (2012) 449–456.
- [14] M.S. Aw, D. Losic, Ultrasound enhanced release of therapeutics from drug-releasing implants based on titania nanotube arrays, *Int. J. Pharm.* 443 (2013) 154–162.
- [15] Y. Hu, K. Cai, Z. Luo, D. Xu, D. Xie, Y. Huang, et al., TiO₂ nanotubes as drug nanoreservoirs for the regulation of mobility and differentiation of mesenchymal stem cells, *Acta Biomater.* 8 (2012) 439–448.
- [16] C.J. Frandsen, K. Noh, K.S. Brammer, G. Johnston, S. Jin, Hybrid micro/nanotopography of a TiO₂ nanotube-coated commercial zirconia femoral knee implant promotes bone cell adhesion in vitro, *Mater. Sci. Eng. C Mater. Biol. Appl.* 33 (2013) 2752–2756.
- [17] H. Tiainen, J.C. Wohlfahrt, A. Verket, S.P. Lyngstadaas, H.J. Haugen, Bone formation in TiO₂ bone scaffolds in extraction sockets of minipigs, *Acta Biomater.* 8 (2012) 2384–2391.
- [18] K.C. Popat, L. Leoni, C.A. Grimes, T.A. Desai, Influence of engineered titania nanotubular surfaces on bone cells, *Biomaterials* 28 (2007) 3188–3197.
- [19] S. Bauer, J. Park, K. von der Mark, P. Schmuki, Improved attachment of mesenchymal stem cells on super-hydrophobic TiO₂ nanotubes, *Acta Biomater.* 4 (2008) 1576–1582.
- [20] K.S. Brammer, S. Oh, C.J. Cobb, L.M. Bjursten, H. van der Heyde, S. Jin, Improved bone-forming functionality on diameter-controlled TiO₂ nanotube surface, *Acta Biomater.* 5 (2009) 3215–3223.
- [21] S. Beke, F. Anjum, H. Tsushima, L. Ceseracciu, E. Chierigatti, A. Diaspro, et al., Towards excimer-laser-based stereolithography: a rapid process to fabricate rigid biodegradable photopolymer scaffolds, *J. R. Soc. Interface* 9 (2012) 3017–3026.
- [22] F. Brandi, F. Anjum, L. Ceseracciu, A.C. Barone, A. Athanassiou, Rigid biodegradable photopolymer structures of high resolution using deep-UV laser photocuring, *J. Micromech. Microeng.* (2011) 21.
- [23] S. Beke, F. Anjum, L. Ceseracciu, I. Romano, A. Athanassiou, A. Diaspro, et al., Rapid fabrication of rigid biodegradable scaffolds by excimer laser mask projection technique: a comparison between 248 and 308 nm, *Laser Phys.* 23 (2013).
- [24] S. Beke, B. Farkas, I. Romano, F. Brandi, 3D scaffold fabrication by mask projection excimer laser stereolithography, *Opt. Mater. Express* (2014).
- [25] S. Scaglione, R. Barengi, S. Beke, L. Ceseracciu, I. Romano, F. Sbrana, et al., Characterization of a bioinspired elastin–polypropylene fumarate material for vascular prostheses applications, *Proc SPIE* 8792, Optical Methods for Inspection, Characterization, and Imaging of Biomaterials, 2013.
- [26] S.F. Wang, L.C. Lu, M.J. Yaszemski, Bone-tissue-engineering material poly(propylene fumarate): correlation between molecular weight, chain dimensions, and physical properties, *Biomacromolecules* 7 (2006) 1976–1982.
- [27] S. Beke, L. Korosi, A. Scarpellini, F. Anjum, F. Brandi, Titanate nanotube coatings on biodegradable photopolymer scaffolds, *Mater. Sci. Eng. C Mater. Biol. Appl.* 33 (2013) 2460–2463.
- [28] L. Korosi, S. Papp, V. Hornok, A. Oszko, P. Petrik, D. Patko, et al., Titanate nanotube thin films with enhanced thermal stability and high-transparency prepared from additive-free sols, *J. Solid State Chem.* 192 (2012) 342–350.
- [29] P.X. Lan, J.W. Lee, Y.J. Seol, D.W. Cho, Development of 3D PPF/DEF scaffolds using micro-stereolithography and surface modification, *J. Mater. Sci. Mater. Med.* 20 (2009) 271–279.
- [30] S. Bauer, J. Park, J. Faltenbacher, S. Berger, K. von der Mark, P. Schmuki, Size selective behavior of mesenchymal stem cells on ZrO₂ and TiO₂ nanotube arrays, *Integr. Biol.* 1 (2009) 525–532.
- [31] J. Park, S. Bauer, K.A. Schlegel, F.W. Neukam, K. von der Mark, P. Schmuki, TiO₂ nanotube surfaces: 15 nm — an optimal length scale of surface topography for cell adhesion and differentiation, *Small* 5 (2009) 666–671.
- [32] S. Zhang, J. Sun, Y. Xu, S. Qian, B. Wang, F. Liu, et al., Biological behavior of osteoblast-like cells on titania and zirconia films deposited by cathodic arc deposition, *Biointerphases* 7 (2012) 60.
- [33] A. Polini, D. Pisignano, M. Parodi, R. Quarto, S. Scaglione, Osteoinduction of human mesenchymal stem cells by bioactive composite scaffolds without supplemental osteogenic growth factors, *PLoS One* 6 (2011).